JOURNAL OF VIROLOGY, Apr. 2007, p. 3109–3123 Vol. 81, No. 7
0022-538X/07/$08.00+0 doi:10.1128/JVI.02124-06

Human Cytomegalovirus UL38 Protein Blocks Apoptosis▽

Scott Terhune,[2]† Emi Torigoi,[1]† Nathaniel Moorman,[2] Maria Silva,[2]‡ Zhikang Qian,[1] Thomas Shenk,[2] and Dong Yu[1]*

Department of Molecular Microbiology, Washington University School of Medicine, Saint Louis, Missouri 63110,[1] *and Department of Molecular Biology, Princeton University, Princeton, New Jersey 08544*[2]

Received 27 September 2006/Accepted 19 December 2006

Apoptosis is an innate cellular defense response to viral infection. The slow-replicating human cytomegalovirus (HCMV) blocks premature death of host cells prior to completion of the infection cycle. In this study, we report that the HCMV UL38 gene encodes a cell death inhibitory protein. A mutant virus lacking the pUL38 coding sequence, AD*dl*UL38, grew poorly in human fibroblasts, failed to accumulate viral DNA to wild-type levels, and induced excessive death of infected cells. Cells expressing pUL38 were resistant to cell death upon infection and effectively supported the growth of AD*dl*UL38. Cells infected with the pUL38-deficient virus showed morphological changes characteristic of apoptosis, including cell shrinkage, membrane blebbing, vesicle release, and chromatin condensation and fragmentation. The proteolytic cleavage of two key enzymes involved in apoptosis, namely, caspase 3 and poly(ADP-ribose) polymerase, was activated upon AD*dl*UL38 infection, and the cleavage was blocked in cells expressing pUL38. The pan-caspase inhibitor Z-VAD-FMK largely restored the growth of AD*dl*UL38 in normal fibroblasts, indicating that the defective growth of the mutant virus mainly resulted from premature death of host cells. Furthermore, cells expressing pUL38 were resistant to cell death induced by a mutant adenovirus lacking the antiapoptotic E1B-19K protein or by thapsigargin, which disrupts calcium homeostasis in the endoplasmic reticulum. Taken together, these results indicate that the HCMV protein pUL38 suppresses apoptosis, blocking premature death of host cells to facilitate efficient virus replication.

Human cytomegalovirus (HCMV), the prototypic betaherpesvirus, is a ubiquitous human pathogen infecting the majority of the world population. Although usually asymptomatic in healthy individuals, HCMV infection causes severe disease in immunocompromised individuals, such as AIDS patients and patients undergoing bone marrow or solid organ transplantation. HCMV is a leading viral cause of birth defects leading to mental retardation and hearing loss (reviewed in reference 8). Additionally, HCMV has been implicated as a possible cofactor in the development of vascular disease (18, 22, 26, 30, 44, 45, 54).

HCMV has a characteristically long replication period, requiring 48 to 72 h to begin producing progeny at peak levels in fibroblasts. Furthermore, cultured cells support continuous virus production for an extended period after completion of the initial infection cycle (reviewed in reference 29). Thus, HCMV is likely to encounter a large array of innate immune responses during its extended replication cycle, which the host cells put forth to control the pathogen. Virtually all viruses have evolved mechanisms to thwart the cellular defenses instituted by the host upon infection. One critical selective pressure is the modulation of apoptosis, an innate antiviral mechanism that is activated by both the direct cellular response and the host immune system to prevent the production of progeny virus upon infection (reviewed in reference 4).

Apoptosis results in the death of infected cells, thus stopping viral spread and preventing persistent infection. The cellular events leading to apoptosis are generally classified into the following three pathways: the mitochondrion-mediated intrinsic pathway, the extracellular ligand-mediated extrinsic pathway, and the endoplasmic reticulum (ER)-mediated pathway (reviewed in references 4 and 7). Most of these pathways promote cell death through activation of caspase cascades. In the intrinsic pathway, sensitized internal cell stress sensors, such as p53, trigger the signaling cascade, leading to the release of proapoptotic factors such as cytochrome *c* from mitochondria, and promote proteolytic activation of caspase 9. In the extrinsic pathway, immune effector cells (e.g., natural killer cells, dendritic cells, and cytotoxic T lymphocytes) transmit signals (e.g., Fas ligand, tumor necrosis factor alpha, and TRAIL) to virus-infected cells via the death receptors and eventually lead to proteolytic activation of caspases 8 and 10. In the ER-mediated pathway, stress signals, such as excessive amounts of unfolded proteins in the ER, trigger the activation of caspases 7, 9, and 12 (31, 32). These three pathways converge on the proteolytic activation of effector caspases and subsequent cleavage of downstream substrates, leading to genome fragmentation, cytoskeletal disintegration, metabolic dysfunction, and ultimately, cell death. These three pathways, however, are intertwined cellular processes. The intrinsic and extrinsic pathways cross talk through cleavage and activation of Bid, which subsequently amplifies the apoptosis signal transmitted from the extrinsic pathway through the mitochondrial arm. In addition to initiating

* Corresponding author. Mailing address: Department of Molecular Microbiology, Washington University School of Medicine, Saint Louis, MO 63110. Phone: (314) 362-7367. Fax: (314) 362-1232. E-mail: dongyu@borcim.wustl.edu.

† S.T. and E.T. contributed equally to this work.

‡ Present address: Department of Pathology, University of Texas Medical Branch, 301 University Boulevard, Galveston, TX 77555-0436.

▽ Published ahead of print on 3 January 2007.

caspase activation, the ER stress signal acts on the mitochondria through members of the Bcl-2 protein family to propagate apoptotic events.

Many viruses, including herpesviruses, modulate cellular apoptosis pathways to facilitate their replication. Upon infection, HCMV and its murine counterpart, murine cytomegalovirus, block apoptosis in various cell types, such as fibroblasts, macrophages, and endothelial cells (5, 10, 21, 27, 28, 46). Furthermore, HCMV is able to inhibit apoptosis induced by a variety of stimuli, including Fas ligand, tumor necrosis factor alpha, and growth factor withdrawal, as well as by infection with an E1B-19K-deficient adenovirus (16, 21, 42, 55). It is conceivable that suppression of apoptosis in host cells is an integral part of the overall strategy adopted by HCMV to evade the host antiviral immunity and is therefore likely to play an important role in virus replication and persistence.

A survey of the HCMV genome failed to identify any viral homologues to known cellular and viral apoptosis regulators (11, 12, 29). Nevertheless, four HCMV gene products, IE1, IE2, pUL36, and pUL37x1, have been shown to block apoptosis in cells overexpressing their genes. IE1 and IE2 protect cells from apoptosis through the cellular kinase Akt-mediated pathway (23, 53, 55). pUL36 interferes with the death ligand-mediated apoptosis pathway at the step upstream of caspase 8 activation (42). pUL37x1 suppresses apoptosis by disrupting the mitochondrial network as well as by sequestering the pro-apoptotic protein Bax (3, 16, 25, 35). Fibroblasts infected with mutant viruses lacking functional pUL36 or pUL37x1 showed reduced levels of resistance to apoptosis, consistent with the role of these two proteins as suppressors of apoptosis (24, 38, 42).

In a prior study, we constructed a comprehensive mutant library in HCMV strain AD169 where every uncharacterized HCMV gene was disrupted by transposon insertion or substitution, and we identified a subset of viral genes that are required for maximal virus replication in human fibroblasts (51). Subsequently, we observed that viruses lacking the UL38 gene induced excessive cell death upon infection of human fibroblasts. In this report, we present evidence that the UL38 gene encodes a new member of the family of cell death inhibitory proteins produced by HCMV, and we demonstrate that its expression is necessary for efficient virus replication.

MATERIALS AND METHODS

Plasmids, retroviral vectors, and antibodies. pGS284-based shuttle vectors pYD-C253, pYD-C215, and pYD-C214 were used for allelic exchange to create recombinant infectious bacterial artificial chromosome (BAC)-based clones carrying the genome of HCMV (AD169) (43, 52). pYD-C253 contained 1.0-kb viral sequences immediately upstream and downstream of the pUL38 open reading frame (ORF). pYD-C215 contained a 2.1-kb viral sequence spanning the pUL38 ORF and its 500-bp upstream and downstream sequences. In pYD-C214, the 1.5-kb XbaI fragment from pGET007, which contained the simian virus 40 early promoter-driven green fluorescent protein (GFP) expression cassette, was inserted between the 1.0-kb US2-US3 sequence and the 1.0-kb US7-US9 sequence (49). pYD-C163, pYD-C160, pYD-C239, and pYD-C258 are retroviral vectors. pYD-C163 and pYD-C160 are pRetro-EBNA-based vectors containing the ORFs of pUL38 and GFP, respectively (20). The retroviral vector pYD-C239 was made by cloning the internal ribosome entry site 2 (IRES2) sequence from pIRES2-EGFP (Clontech) and the dsRed coding sequence from pDsRED-N1 (Clontech) into BglII/NotI sites of pLPCX (Clontech). pYD-C258 was created by cloning the pUL38 ORF upstream of the IRES2 site of pYD-C239. The fidelity of all PCR products was confirmed by sequencing.

To generate a monoclonal antibody to pUL38, nucleotides 105 to 996 of the pUL38 ORF were cloned downstream of a six-His tag in the expression vector pQE (QIAGEN). The fusion protein was produced in *Escherichia coli*, purified using Ni-agarose beads, and used as an immunogen to generate murine hybridomas. The anti-pUL38 antibody, 8D6, was identified by screening against His-pUL38 or His-YY1 as a control in enzyme-linked immunosorbent assays. Additional primary antibodies used in this study included anti-IE1 (1B12; A. Marchini, P. Robinson, and T. Shenk, unpublished data), anti-pp28 (41), anti-β-actin (AC15; Abcam), anti-α-tubulin (DM1A; Sigma), anti-caspase 3 (Asp175) (MAB835; R&D Systems), and anti-poly(ADP-ribose) polymerase (anti-PARP) (Asp214) (19F4; Cell Signaling).

Cells and viruses. Primary human foreskin fibroblasts (HF), human MRC-5 embryonic lung cells, and HeLa cells were propagated in Dulbecco's modified Eagle medium supplemented with 10% fetal calf serum. To create HF cells expressing pUL38 or GFP, the retrovirus stocks *retro*-UL38 and *retro*-GFP were made by transfecting the retroviral vectors pYD-C163 and pYD-C160, respectively, into Phoenix Ampho cells (20). HF cells were transduced with *retro*-UL38 or *retro*-GFP three times to generate a population of cells expressing pUL38 or GFP. To create HeLa cell lines stably expressing pUL38/dsRed or dsRed only, HeLa cells were transfected with pYD-C258 or pYD-C239, respectively, using Lipofectamine 2000 (Invitrogen), and were selected with 1 μg/ml puromycin. Individual puromycin-resistant colonies were trypsinized and subcloned in the presence of 1 μg/ml puromycin. The expression of pUL38 from transduced HF cells and from stable HeLa cell lines was confirmed by Western blotting using the monoclonal antibody 8D6. Expression of GFP or dsRed from control cells was validated by fluorescence microscopy analysis.

The GFP-expressing wild-type BAC clone pAD-GFP was constructed by replacing the viral US4-US6 region with the GFP expression cassette, using allelic exchange with the shuttle vector pYD-C214 and pAD/Cre (52). Recombinant BAC clones pAD*dl*UL38 and pAD*dl*UL38-GFP, which lacked the entire pUL38 ORF, were created by performing allelic exchange with the shuttle vector pYD-C253 on pAD/Cre and pAD-GFP, respectively. Marker-rescued BAC clones pAD*rev*UL38 and pAD*rev*UL38-GFP, in which the UL38 allele was repaired, were created by performing allelic exchange with the shuttle vector pYD-C215 on pAD*dl*UL38 and pAD*dl*UL38-GFP, respectively. To reconstitute wild-type viruses (AD*wt* and AD*wt*-GFP) and marker-rescued UL38 revertants (AD*rev*UL38 and AD*rev*UL38-GFP), 2 μg of the corresponding BAC DNA and 1 μg of the pp71 expression plasmid were transfected into HF cells by electroporation as previously described (52). To reconstitute UL38 mutant viruses (AD*dl*UL38 and AD*dl*UL38-GFP), UL38 recombinant BAC DNA was transfected into pUL38-expressing fibroblasts by electroporation. The culture medium was changed at 24 h posttransfection, and the cell-free culture supernatant was harvested as a virus stock when the entire monolayer of cells was lysed.

Virus stocks were produced either directly from transfection of BAC DNA or from infection at a multiplicity of 0.01 PFU/cell. Infected cell culture media were cleared of cell debris by low-speed centrifugation and collected as stocks of cell-free virus. In general, virus titers were determined in duplicate by a plaque assay with pUL38-expressing fibroblasts, unless otherwise noted (52). To determine virus titers by IE1 expression, viruses were collected from both cell-free supernatants and infected cells at various time points postinfection. Cell-associated virus was isolated through three rounds of freezing and thawing in a dry ice and ethanol bath. Serial dilutions of virus samples were plated on MRC-5 cells. At 36 h postinfection, infected cells were fixed and permeabilized in methanol at −20°C for 15 min. IE1-positive cells were labeled using the primary mouse antibody to IE1 (1B12) and the secondary goat anti-mouse antibody conjugated with Alexa Fluor 546 (Molecular Probes), and positive cells were quantified at the appropriate dilution using a fluorescence microscope.

To determine DNA levels in virus stocks, real-time PCR was performed, using 100 μl of either cell-free virus stock or virus stock that was partially purified by centrifugation through a 20% sorbitol cushion. The pelleted virus was resuspended in phosphate-buffered saline (PBS). To remove free DNA, samples were treated with DNA-free reagents (Ambion) and then lysed in lysis buffer (400 mM NaCl, 10 mM Tris [pH 8.0], 10 mM EDTA, 0.1 mg/ml protease K, 0.2% sodium dodecyl sulfate [SDS]) at 37°C overnight. To determine DNA levels in infected cells, cells were harvested, pelleted, resuspended in lysis buffer, and incubated at 37°C overnight. For all samples, DNAs were extracted with phenol-chloroform, treated with RNase A, extracted again with phenol-chloroform, and precipitated with ethanol. DNAs were resuspended in water and quantified by real-time PCR analysis using TagMan probes (Applied Biosystems) and primers specific for the UL123 gene or cellular β-actin, as previously described (17). In some experiments, an additional UL123-specific TaqMan probe (5′-VIC-TCCGTCTGGGT ATATTTTTTCAGC-6-carboxytetramethylrhodamine-3′) (Applied Biosystems) and pair of primers (5′-GGCGCCAGTGAATTTCTC-3′ and 5′-TGCGGCAT AGAATCAAGGA-3′) were also used.

Analysis of intracellular viral RNA and protein. To determine RNA levels in infected cells by real-time reverse transcription-PCR (RT-PCR), total RNA was isolated using Trizol reagent (Invitrogen) following the manufacturer's instructions, and contaminating DNA was removed using DNA-free reagents (Ambion). Relative quantitation was accomplished through two-step real-time RT-PCR, as previously described (48). Briefly, cDNAs were synthesized with TaqMan reverse transcription reagents and random hexamers according to the manufacturer's instructions (Applied Biosystems). Real-time PCR was completed with SYBR green PCR master mix (Applied Biosystems) and primers specific to exon 4 of UL123 (5′-GCCTTCCCTAAGACCACCAAT-3′ and 5′-ATTTTCTGGGCATAAGCCATAATC-3′), UL99 (5′-GTGTCCCATTCCCGACTCG-3′ and 5′-TTCACAACGTCCACCCACC-3′), or glyceraldehyde-3-phosphate dehydrogenase (GAPDH) (5′-CTGTTGCTGTAGCCAAATTCGT-3′ and 5′-ACCCACTCCTCCACCTTTGAC-3′).

To analyze proteins by Western blotting, infected cells were scraped into medium and collected by centrifugation at 1,000 rpm at 4°C for 5 min. Cell pellets were washed with PBS and lysed in SDS sample buffer (0.05 mM Tris-HCl [pH 6.8], 2% SDS, 10% glycerol, 0.1% bromophenol blue, 1.25% [vol/vol] 2-mercaptoethanol). Lysates from equal cell numbers were run in a sodium dodecyl sulfate-containing 10% polyacrylamide gel. Resolved proteins were transferred to polyvinylidene difluoride membranes, and membranes were blocked with 5% nonfat milk in Tris-buffered saline containing 0.05% Tween 20. Proteins were labeled with the primary antibodies listed above and incubated with a secondary goat anti-mouse antibody (Amersham). Antibodies were visualized by ECL-Plus detection (Amersham) and quantified by scanning membranes with a Fuji FLA5000 autoimaging analyzer or a Molecular Dynamics Storm phosphorimager.

To analyze proteins by immunofluorescence, cells were grown on glass coverslips, the medium was removed at various times postinfection, and cells were washed once with PBS and fixed in 2% paraformaldehyde for 20 min. Fixed cells were washed twice with PBS and permeabilized with 1 mg/ml Zwittergent for 1 min. Cells were washed twice with PBS, incubated in blocking solution (5% fetal calf serum in PBS) for 20 min, and then labeled with the primary antibody in blocking solution for 20 min. Cells were washed again and then incubated with the secondary antibody in blocking solution for 20 min. Cells were then washed three times with PBS, rinsed once with H_2O, and mounted on slides with Slow-Fade Gold solution containing DAPI (4′,6′-diamidino-2-phenylindole) to counterstain DNA (Molecular Probes). Images were captured using Axiovision software with a Zeiss Axioskop 2 MOT Plus fluorescence microscope or a Zeiss LSM510 confocal microscope.

Cell death/apoptosis assays. HF or HeLa cells were infected with recombinant HCMV or the mutant adenovirus *dl*337, treated with 0.2 μg/ml α-Fas antibody (7C11; Coulter) and 10 μg/ml cycloheximide (Sigma) for 10 h and 20 h, or treated with 2 μM thapsigargin (16, 34, 39, 42). The morphology of infected cells was examined under a phase-contrast or fluorescence microscope at different times postinfection. Dying cells were detached from the culture dish and fragmented, while surviving cells remained attached and maintained a flat morphology. To quantify the number of surviving cells in each infected culture, viable cells attached to the culture dish were labeled with DAPI and counted in four to six independent fields for each sample under a fluorescence microscope. Alternatively, attached cells from infected cultures were collected, and cell numbers were measured by flow cytometry relative to an internal control.

Several assays were used to examine characteristic cellular events associated with apoptosis. To visualize chromatin condensation and fragmentation, cells were grown on coverslips, fixed in 2% paraformaldehyde, and permeabilized in 1 mg/ml Zwittergent. DNA strand breaks were labeled with a terminal deoxynucleotidyltransferase-mediated dUTP-biotin nick end labeling (TUNEL) kit (Roche). Cells were mounted on slides with Slow-Fade Gold solution containing DAPI (Molecular Probes). The morphology of chromatin-labeled and TUNEL-positive cells was examined by fluorescence microscopy. To analyze proteolytic cleavage of caspase 3 and PARP, infected cells were harvested, proteins were separated by electrophoresis, and cleaved forms of caspase 3 and PARP were detected by Western blotting, using ECL-Plus detection. Jurkat cell lysates treated with 0.25 mg/ml cytochrome *c* were prepared according to the manufacturer's instructions (Cell Signaling) and used as the positive control for caspase 3 and PARP cleavage. To investigate the effect of cell death on virus growth, normal HF cells were infected with recombinant HCMV at an input genome number equivalent to 2 PFU of wild-type virus/cell in the presence of 100 μM pan-caspase inhibitor Z-VAD-FMK, which was initially made as a 20 mM stock solution in dimethyl sulfoxide (DMSO; Calbiochem). Every 24 h, the culture medium was collected, and infected cells were refed with the appropriate Z-VAD-FMK- or DMSO-containing fresh medium. The yields of cell-free virus in culture medium were determined by a plaque assay with pUL38-expressing HF cells.

RESULTS

Construction of recombinant BAC-HCMV clones carrying alteration in the pUL38 coding sequence. The UL36-UL38 region of HCMV encodes multiple transcripts (Fig. 1A). UL38 is located within the intron of the UL37 gene, which encodes three proteins, pUL37x1, pUL37, and pUL37M, due to alternative splicing. pUL37 and pUL37M are dispensable for HCMV replication in human fibroblasts (6, 16). pUL37x1 is required for replication of the HCMV AD169 strain but is dispensable for the Towne strain, and therefore its requirement is strain specific (24, 38, 51). To study the function of pUL38 in virus infection, we constructed recombinant viruses lacking the entire pUL38 coding sequence. Two parental BAC-HCMV clones, pAD/Cre and pAD-GFP, were used as wild-type viruses in this study: pAD/Cre carries the full-length genome of HCMV strain AD169 (52), and its derivative, pAD-GFP, carries a simian virus 40 early promoter-driven GFP gene in place of the viral US4-US6 region. Viruses derived from both BAC clones (AD*wt* and AD*wt*-GFP) grew indistinguishably from the parental AD169 virus (52; data not shown). Deletion of UL38 was done by using the BAC-based genetic approach (52). pAD*dl*UL38 and pAD*dl*UL38-GFP, derived from pAD/Cre and pAD-GFP, respectively, lack the entire pUL38 coding sequence and were used to generated pUL38-deficient viruses (AD*dl*UL38 and AD*dl*UL38-GFP, respectively). The UL38 loci in pAD*dl*UL38 and pAD*dl*UL38-GFP were subsequently repaired, producing the marker-rescued BAC clones pAD*rev*UL38 and pAD*rev*UL38-GFP, respectively, which were used to generate revertant viruses (AD*rev*UL38 and AD*rev*UL38-GFP). Recombinant BAC clones were examined for integrity by using EcoRI and BamHI restriction endonuclease digestion (Fig. 1B), PCR, and Southern blot analysis (Fig. 1C). The 6,380-bp EcoRI fragment containing the UL38 sequence in pAD/Cre and pAD*rev*UL38 was reduced to a 5,402-bp fragment in pAD*dl*UL38 due to UL38 deletion (Fig. 1B, lanes 1 to 3). The deletion of UL38 was confirmed by BamHI digestion. As expected, pAD*dl*UL38 lost the 5,029-bp fragment but gained the 5,219-bp fragment that comigrated with the 5,242-bp fragment, as seen for pAD/Cre and pAD*rev*UL38 (lanes 4 to 6). pAD-GFP was identical to pAD/Cre except for the replacement of the viral US4-US6 sequence with the GFP expression cassette. Compared to pAD/Cre, pAD-GFP had a unique EcoRI fragment of 11.2 kb and two BamHI fragments, of 8,216 bp and 7,950 bp, and in the meantime, pAD-GFP lost an EcoRI fragment of 12.4 kb and two BamHI fragments, of 6,982 bp and 10,402 bp (lanes 7, 8, 11, and 12). Similarly, the EcoRI and BamHI restriction patterns of pAD*dl*UL38-GFP were completely consistent with expectations (compare lane 10 with lane 1 and lane 14 with lane 4). A more complex pattern arose when pAD*rev*UL38-GFP was examined. The restriction patterns of pAD*rev*UL38-GFP were similar to those of pAD-GFP except that the BamHI fragment of 8,090 bp and the EcoRI fragment of 11,083 bp spanning the viral UL58-UL68 region in pAD/Cre sustained a small internal deletion when pAD*rev*UL38-GFP was constructed. As a result, the sizes of these two fragments in

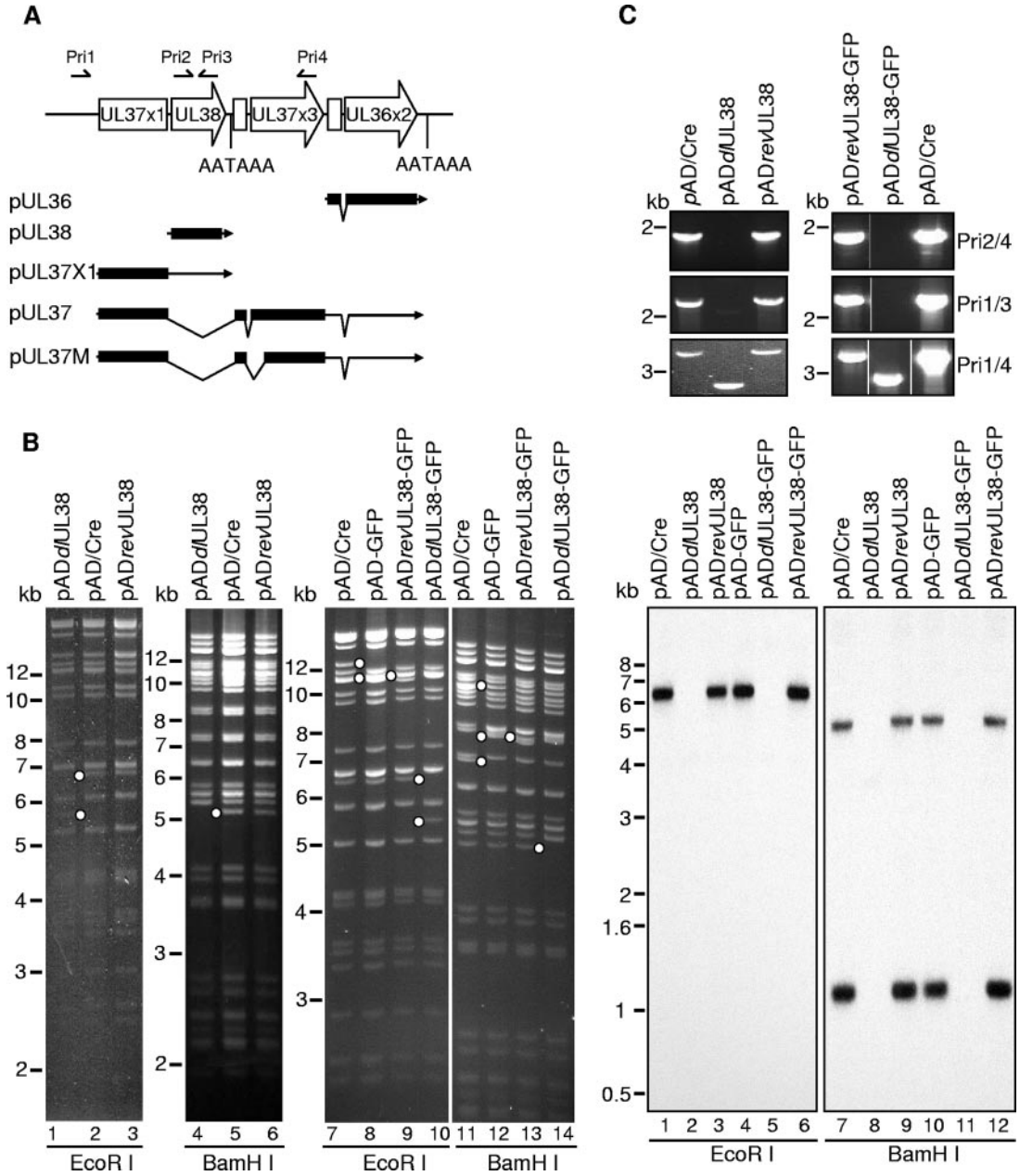

FIG. 1. Construction of UL38 recombinant BAC-HCMV clones. (A) Viral genomic region carrying UL36-UL38. The first line represents the schematic structure of the viral genomic sequence. The coding sequences of pUL36, pUL37, and pUL38 are indicated by block arrows. The C terminus of each ORF is indicated by the direction of the arrow. Also indicated are the locations of two poly(A) signals immediately downstream of the pUL38 and pUL36 coding sequences and four primers used for PCR amplification to validate sequence alteration introduced in UL38 recombinant BAC-HCMV clones. The 3′ ends of the primers are indicated by the directions of the arrows. The next five lines represent UL36-, UL37-, and UL38-related transcripts. The 3′ end of each transcript is indicated by the direction of the arrow. (B) EcoRI and BamHI restriction digestion analysis. (C) PCR and Southern blot analysis of UL38 recombinant BAC-HCMV clones. Each recombinant BAC-HCMV clone analyzed is described in the text. Dots indicate restriction fragments unique to a recombinant BAC clone due to engineered sequence alterations. For PCR analysis, primer pairs used to amplify specific viral sequences are indicated. For Southern blot analysis, a ^{32}P-labeled probe against the UL38 open reading frame was used to hybridize EcoRI- or BamHI-digested BAC-HCMV DNA. Molecular size markers are indicated.

pAD*rev*UL38-GFP were reduced 200 to 300 bp (compare lane 8 with lane 9 and lane 12 with lane 13). Nevertheless, transfection of pAD*rev*UL38-GFP into HF cells efficiently reconstituted a virus that replicated indistinguishably from the wild type (data not shown). Collectively, these data show that the gross genomic integrity of the UL38 mutant BAC clones remained intact.

The UL38 gene loci of the recombinant BAC-HCMV clones were examined further by PCR analysis (Fig. 1C, top panel) and Southern blot analysis (Fig. 1C, bottom panel). For PCR

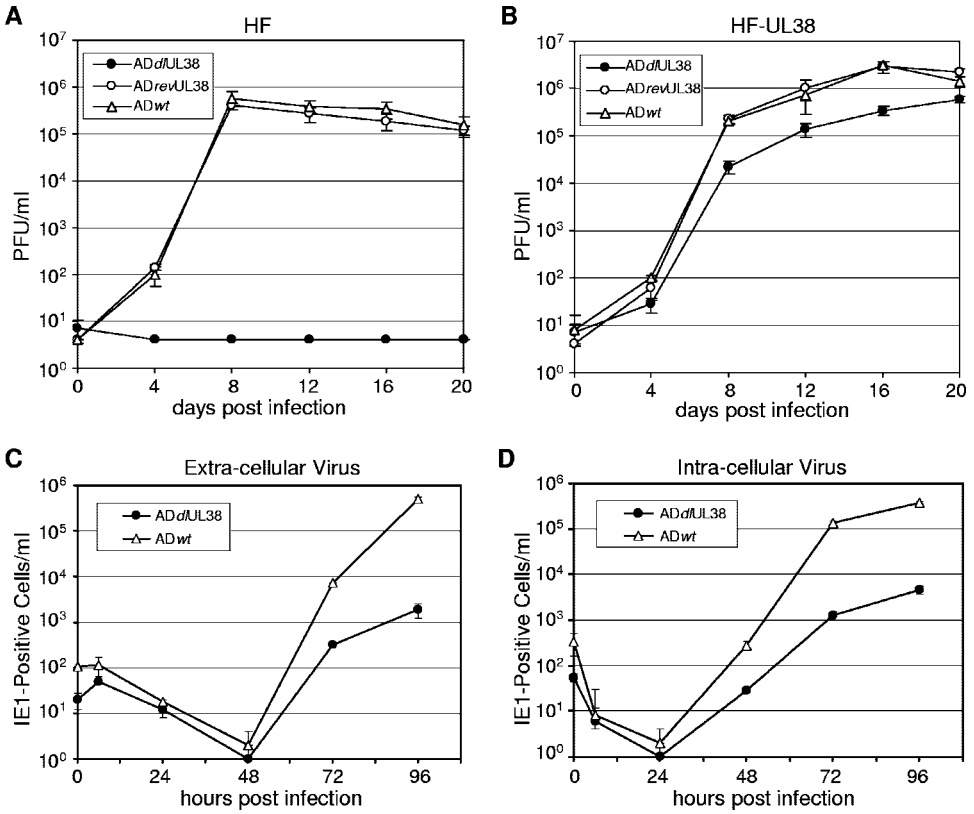

FIG. 2. The marked growth defect of AD*dl*UL38 is restored by the expression of pUL38 in *trans*. Multistep growth analysis was performed with AD*wt*, AD*dl*UL38, and AD*rev*UL38 in normal HF cells (A) and in HF cells transduced with the pUL38-expressing retroviral vector (B). Cells were infected at a multiplicity of 0.01 PFU/cell, culture medium was collected at the indicated times, and yields of cell-free virus were titrated in duplicate by a plaque assay with HF-UL38 cells. Single-step growth analysis of AD*dl*UL38 in MRC-5 cells was performed to examine the production of extracellular virus (C) and intracellular virus (D). MRC-5 cells were infected with AD*dl*UL38 or AD*wt* at an input genome number equivalent to 0.2 PFU of wild-type virus/cell. Infected cell culture medium was collected as extracellular virus samples, and intracellular virus was isolated by freezing and thawing cell pellets. The amount of virus present in each sample was determined by counting the number of IE1-positive cells. The experiment was completed in duplicate.

analysis, a combination of four primers was used: Pri 2 and Pri 3 were located within the pUL38 coding sequence, whereas Pri 1 and Pri 4 were located outside the UL38 flanking sequences that were used to construct recombinants by allelic exchange (Fig. 1A). As expected, PCRs with wild-type or marker-rescued clones and the primer pair Pri 2/Pri 4 or Pri 1/Pri 3 gave rise to a 1.6-kb or 2.3-kb product, respectively. PCRs with UL38 deletion clones and the above primers failed to yield any products due to a lack of binding sites for primers Pri 2 and Pri 3. PCRs with the outside primers Pri 1 and Pri 4 resulted in a 3.5-kb product for wild-type and marker-rescued clones and a 2.5-kb product for UL38 deletion clones. Furthermore, Southern blot analysis using a probe against the entire UL38 open reading frame showed that wild-type and marker-rescued BAC clones contained the predicted set of UL38-specific fragments (i.e., the EcoRI fragment of 6,380 bp [Fig. 1C, bottom panel, lanes 1, 3, 4, and 6] and two BamH1 fragments, of 5,029 bp and 1,168 bp [Fig. 1C, bottom panel, lanes 7, 9, 10, and 12]) that was absent in UL38 deletion BAC clones (Fig. 1C, bottom panel, lanes 2, 5, 8, and 11), indicating that UL38 was reinserted at the single desired location within the genome in the marker-rescued BAC-HCMV clones. Taken together, our data indicate that the recombinant BAC-HCMV clones contained the precise intended modifications in UL38. Finally, all of the modifications in the BAC-HCMV clones were confirmed by direct sequencing.

pUL38 is required for efficient virus replication in fibroblasts. To examine the role of pUL38 in virus replication, we analyzed the growth kinetics of the pUL38-deficient virus, AD*dl*UL38, in human fibroblast cells. The multistep growth of wild-type, deletion mutant, and revertant viruses was examined in normal fibroblasts (Fig. 2A). When HF cells were infected with AD*dl*UL38 at a multiplicity of 0.01 PFU/cell, cell-free progeny virus was not detected for the duration of the assay (20 days). This represents a $>10^5$-fold difference in peak yield of the mutant compared to that of the wild type. In contrast, the revertant AD*rev*UL38 replicated indistinguishably from the wild type. This indicates that the deletion at the UL38 locus is exclusively responsible for the growth defect of AD*dl*UL38.

We also examined the multistep growth of AD*dl*UL38 in pUL38-expressing HF cells (HF-UL38) made by transduction of primary human fibroblasts with a replication-defective retrovirus expressing pUL38 (*retro*-UL38) (Fig. 2B). The $>10^5$-fold difference in peak yield of AD*dl*UL38 compared to that of the wild type in normal HF cells was reduced to 5-fold in HF-UL38 cells. The growth kinetics of the GFP-tagged wild-

type, UL38 mutant, and revertant viruses, i.e., AD*wt*-GFP, AD*dl*UL38-GFP, and AD*rev*UL38-GFP, were similar to those of AD*wt*, AD*dl*UL38, and AD*rev*UL38, respectively (data not shown). Therefore, the substantial complementation of UL38 deletion virus growth in HF-UL38 cells, coupled with the restoration of growth in marker-rescued virus, indicates that the phenotype observed for the UL38 deletion virus results directly and exclusively from the loss of functional UL38.

We then examined the single-step growth kinetics of AD*dl*UL38. In order to appropriately perform this and other experiments that required the use of large amounts of input virus, we determined the ratios of DNA-containing particle to PFU for the mutant stocks relative to that for the wild type (see Materials and Methods). Mutant virus stocks were made by propagating the virus in pUL38-expressing fibroblasts. We were concerned that the infectivity might vary among different batches of mutant stock because of the heterogeneous nature of the pUL38-expressing cells. We examined several batches of the AD*dl*UL38 stocks that were prepared in different batches of pUL38-expressing fibroblasts at different times. As anticipated, the ratios of DNA-containing particles to PFU for these mutant stocks ranged from the wild-type level to as much as 10-fold greater than the wild-type level (data not shown). Consequently, we normalized infection of the UL38 mutant to that of wild-type virus, using equal numbers of DNA-containing particles/cell for the remainder of our studies.

We infected normal fibroblasts with AD*dl*UL38 or AD*wt* at an input genome number equivalent to 0.2 PFU of wild-type virus/cell, collected intracellular and extracellular viruses at various times postinfection, and determined the amount of infectious virus produced at each time point by using a fluorescence assay in which the number of IE1-positive cells was determined at 36 h postinfection (see Materials and Methods). Compared to the wild type, AD*dl*UL38 produced 23- and 265-fold less infectious extracellular virus (Fig. 2C) and 107- and 81-fold less intracellular virus (Fig. 2D) at 72 h and 96 h postinfection, respectively. These data provide additional evidence for a functional role for pUL38 in the efficient replication of HCMV in cultured fibroblasts.

Expression and localization of pUL38 during HCMV infection. We made a monoclonal antibody by using the C-terminal two-thirds of the pUL38 protein as an immunogen and examined the expression of pUL38 by Western blotting (Fig. 3A). A protein of 37 kDa was recognized by the pUL38-specific monoclonal antibody in lysates of wild type-infected cells but not AD*dl*UL38-infected cells. This result indicates that pUL38 is expressed at the predicted size and confirms that AD*dl*UL38 has lost the ability to produce pUL38. Interestingly, although the UL38 gene was classified as an early gene (47), the UL38 protein was detected as early as 6 h postinfection and continued to accumulate throughout the course of infection, with maximum accumulation occurring at 48 h postinfection (Fig. 3A). pUL38 has been identified as a minor virion constituent by a proteomic approach (50); therefore, it is possible that the virion-associated protein contributed, at least in part, to the accumulation of pUL38 that we observed at 6 h postinfection. The subcellular localization of pUL38 during virus infection was examined by immunofluorescence. Consistent with the results of Western blotting, we detected pUL38 within infected cells as early as 8 h postinfection (Fig. 3B). At early

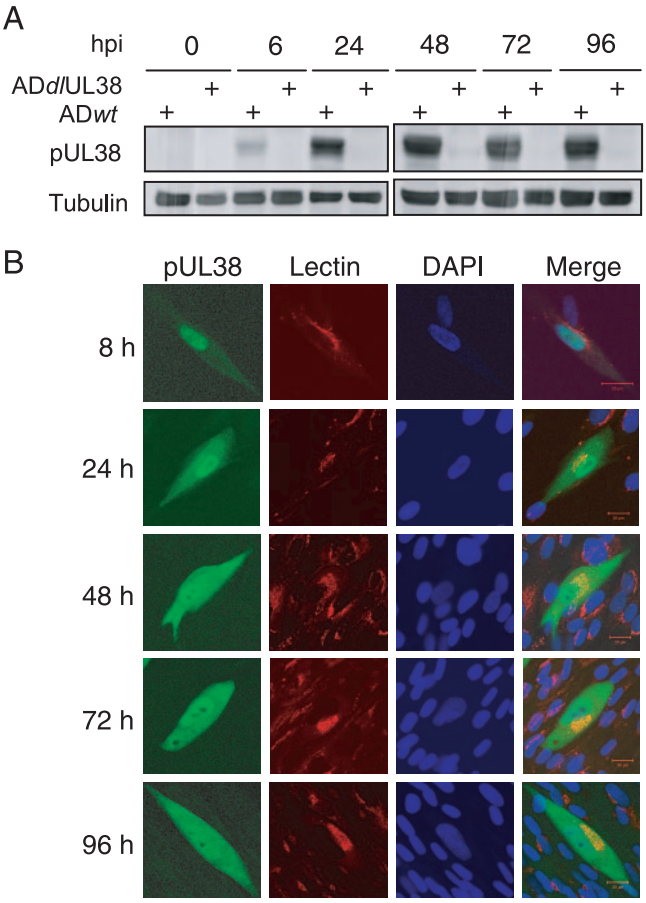

FIG. 3. Expression and subcellular localization of HCMV pUL38. (A) Fibroblasts were infected with AD*dl*UL38 or AD*wt* at an input genome number equivalent to 0.2 PFU of wild-type virus/cell, and cell lysates were analyzed by Western blotting using a pUL38-specific monoclonal antibody at the indicated times. An antibody to alpha-tubulin was used as a loading control. (B) Fibroblasts were infected with AD*wt*, and immunofluorescence was performed to examine the localization of pUL38 at the indicated times (green). Also shown are the Golgi apparatus, defined by the lectin *Helix pomatia* agglutinin (red), the nucleus, defined by DAPI (blue), and the merged images.

times postinfection, pUL38 was predominantly localized in the nucleus, with low levels of diffuse expression throughout the cytoplasm. During the course of infection, the levels of pUL38 increased in both the nuclear and cytoplasmic compartments (Fig. 3B). By 96 h postinfection, similar levels of pUL38 were reached in both compartments. In sum, these data reveal a dynamic subcellular location pattern for the protein in the nucleus and the cytoplasm during the course of infection.

The pUL38 deletion virus fails to accumulate viral DNA to wild-type levels. We next searched for the step in the HCMV replication cycle at which pUL38 is needed for the production of a normal virus yield. We infected normal fibroblasts with AD*dl*UL38 or AD*wt* at an input genome number equivalent to 0.2 PFU of wild-type virus/cell and quantified the viral DNA accumulation relative to cellular β-actin accumulation at different times postinfection. The pUL38-deficient mutant accumulated 42-fold less viral DNA

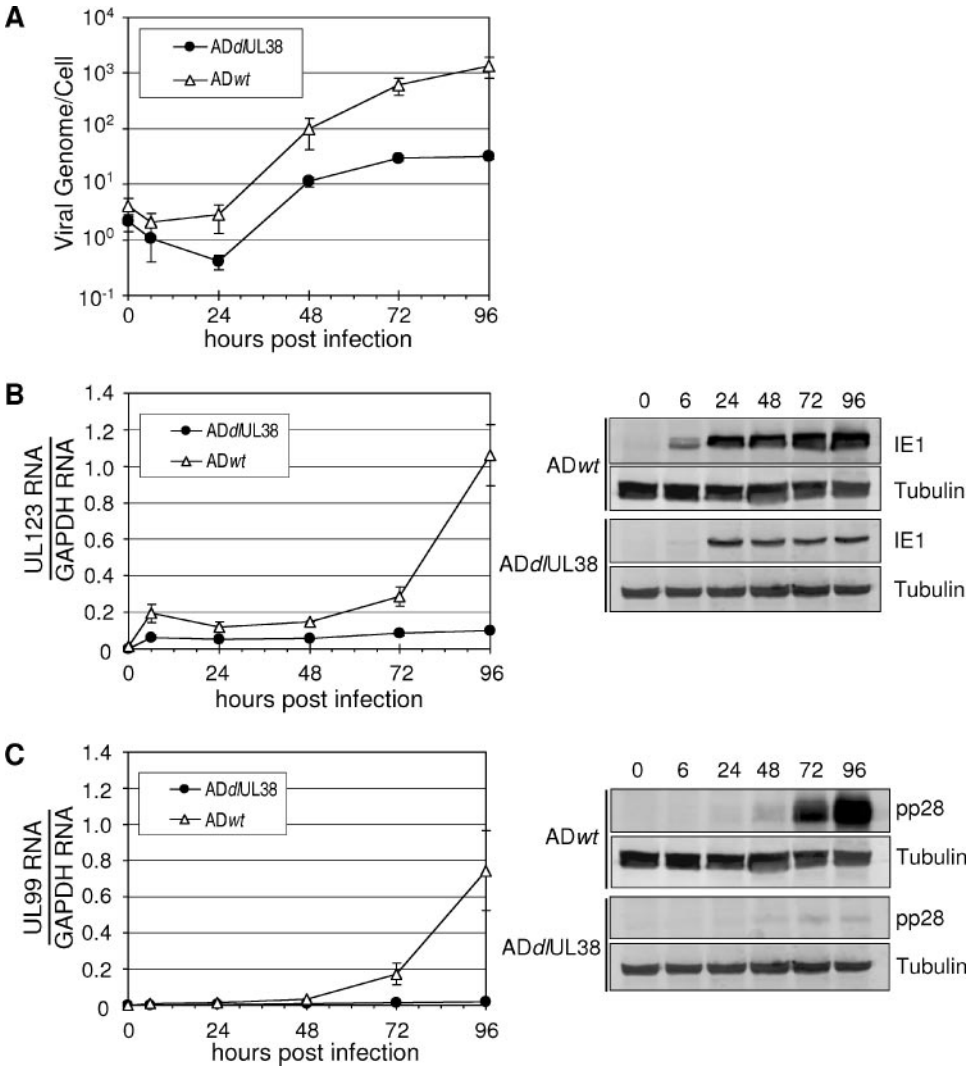

FIG. 4. AD*dl*UL38 fails to replicate viral genomes to wild-type levels. (A) Accumulation of viral DNA. Fibroblasts were infected with AD*dl*UL38 or AD*wt* at an input genome number equivalent to 0.2 PFU of wild-type virus/cell, total cell-associated DNA was isolated, and viral genomes were quantified using real-time PCR and normalized to β-actin DNA. (B) Accumulation of the UL123 transcript and the protein product IE1. Fibroblasts were infected under the conditions described above. Total RNA was isolated at the indicated times postinfection, and UL123 RNA was quantified by real-time RT-PCR using primers specific to UL123, with SYBR green detection, and normalized to GAPDH RNA. Accumulation of the IE1 protein was determined by Western blot analysis. An antibody to alpha-tubulin was used as a loading control. (C) Accumulation of the UL99 transcript and the protein product pp28. The UL99 transcript was measured by real-time RT-PCR using primers specific to UL99. The pp28 protein was detected by Western blot analysis using an antibody to pp28.

than its parent by 96 h postinfection (Fig. 4A). We also monitored the accumulation of the immediate-early UL123 and late UL99 transcripts relative to that of the cellular GAPDH RNA by using real-time RT-PCR. We observed, on average, that twofold less UL123 RNA accumulated in AD*dl*UL38 infection than in wild-type infection between 6 h and 48 h postinfection (Fig. 4B, left panel). We reasoned that this twofold difference was the result of the twofold difference in input viral genomes observed between the two viruses (Fig. 4A, 0 h). The differences in UL123 RNA levels increased at late times postinfection, reaching 10.5-fold at 96 h postinfection. The viral IE1 protein encoded by the UL123 gene accumulated with kinetics similar to that of transcript accumulation (Fig. 4B, right panel). Thus, during the course of virus infection, AD*dl*UL38 expressed IE1 with wild-type kinetics at immediate-early and early times postinfection, and IE1 expression became less efficient after the defect in viral DNA replication was evident. To provide additional evidence for the DNA replication defect in AD*dl*UL38, we examined the expression of the UL99 late gene that encodes pp28. While both the transcript and the protein product of UL99 accumulated maximally at 96 h postinfection in wild-type virus-infected cells, little expression of UL99 was observed at the RNA or protein level in AD*dl*UL38-infected cells throughout the course of infection (Fig. 4C). In sum, the expression of an immediate-early gene is normal, but DNA replication and expression of a late gene are markedly reduced, in the absence of pUL38.

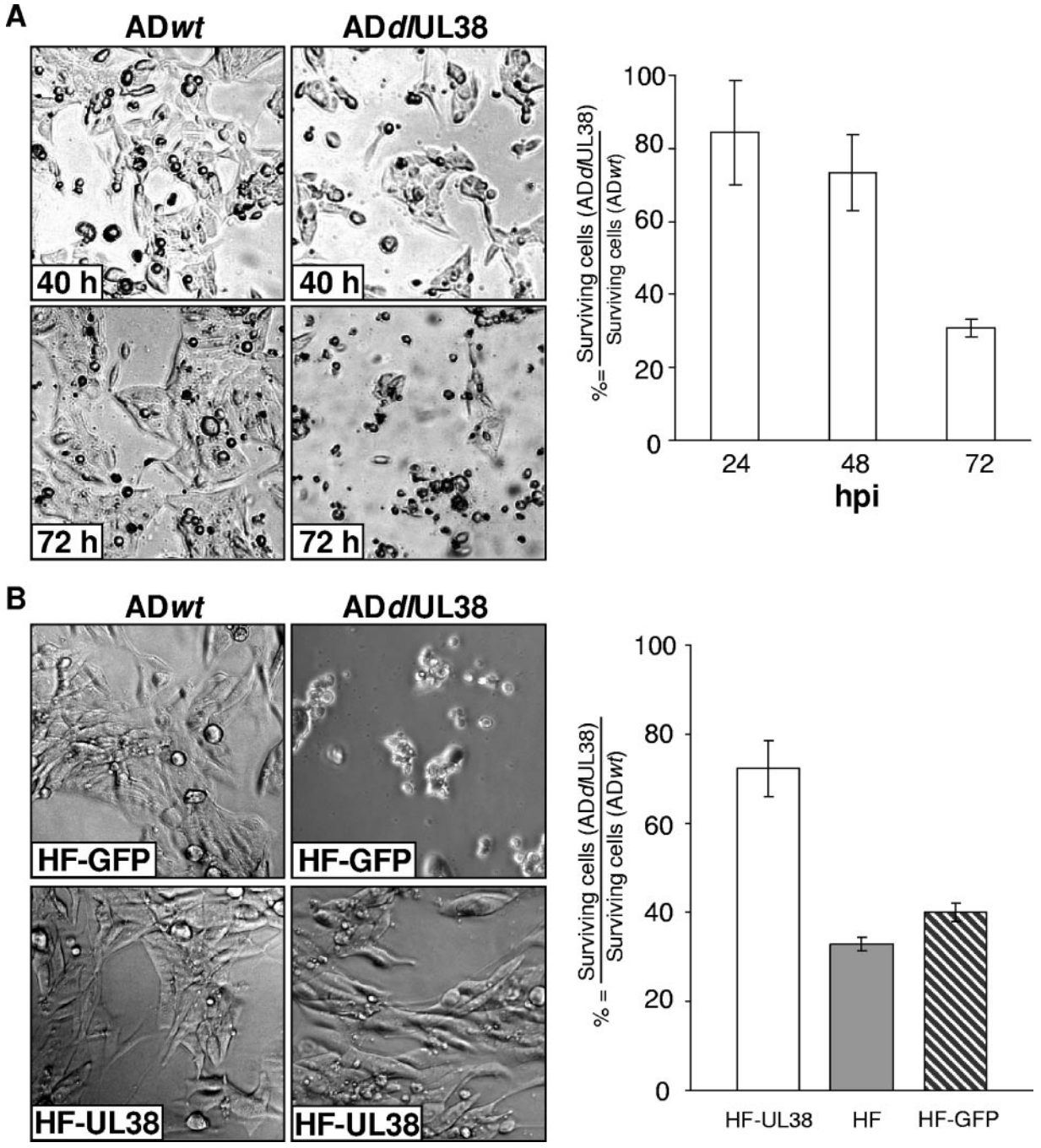

FIG. 5. pUL38 is required to block cell death in HCMV-infected HF cells. (A) For the left panel, normal HF cells were infected with AD*wt* or AD*dl*UL38 at an input genome number equivalent to 2 PFU of wild-type virus/cell, and the morphology of infected cells was examined with a phase-contrast microscope at 40 h and 72 h postinfection. For the right panel, quantitative analysis was performed to compare cell death in HF cells infected with AD*dl*UL38 to that in cells infected with AD*wt*, as described in Materials and Methods. The ratio of the number of viable cells in AD*dl*UL38 infection to that in AD*wt* infection was plotted as a function of hours postinfection (hpi). (B) For the left panel, HF-GFP or HF-UL38 fibroblasts were infected with AD*wt* or AD*dl*UL38 at an input genome number equivalent to 1 PFU of wild-type virus/cell, and cell morphology was examined under a phase-contrast microscope at 72 h postinfection. For the right panel, quantitative analysis was performed to compare cell death in various fibroblasts infected with AD*dl*UL38 to that in cells infected with AD*wt*, as described in Materials and Methods. The ratio of the number of viable cells in AD*dl*UL38 infection to that in AD*wt* infection was plotted for various types of human fibroblasts tested. The results shown are representative of at least two independent experiments.

pUL38 is required for the suppression of premature cell death in HCMV-infected cells. We observed a striking morphological difference between cells infected with wild-type virus and those infected with AD*dl*UL38 (Fig. 5A, left panel). At 40 h postinfection, there was little difference between the two viruses, but at 72 h postinfection, many more AD*dl*UL38-infected than wild-type virus-infected cells had detached from the culture dish, and the cells that remained attached exhibited

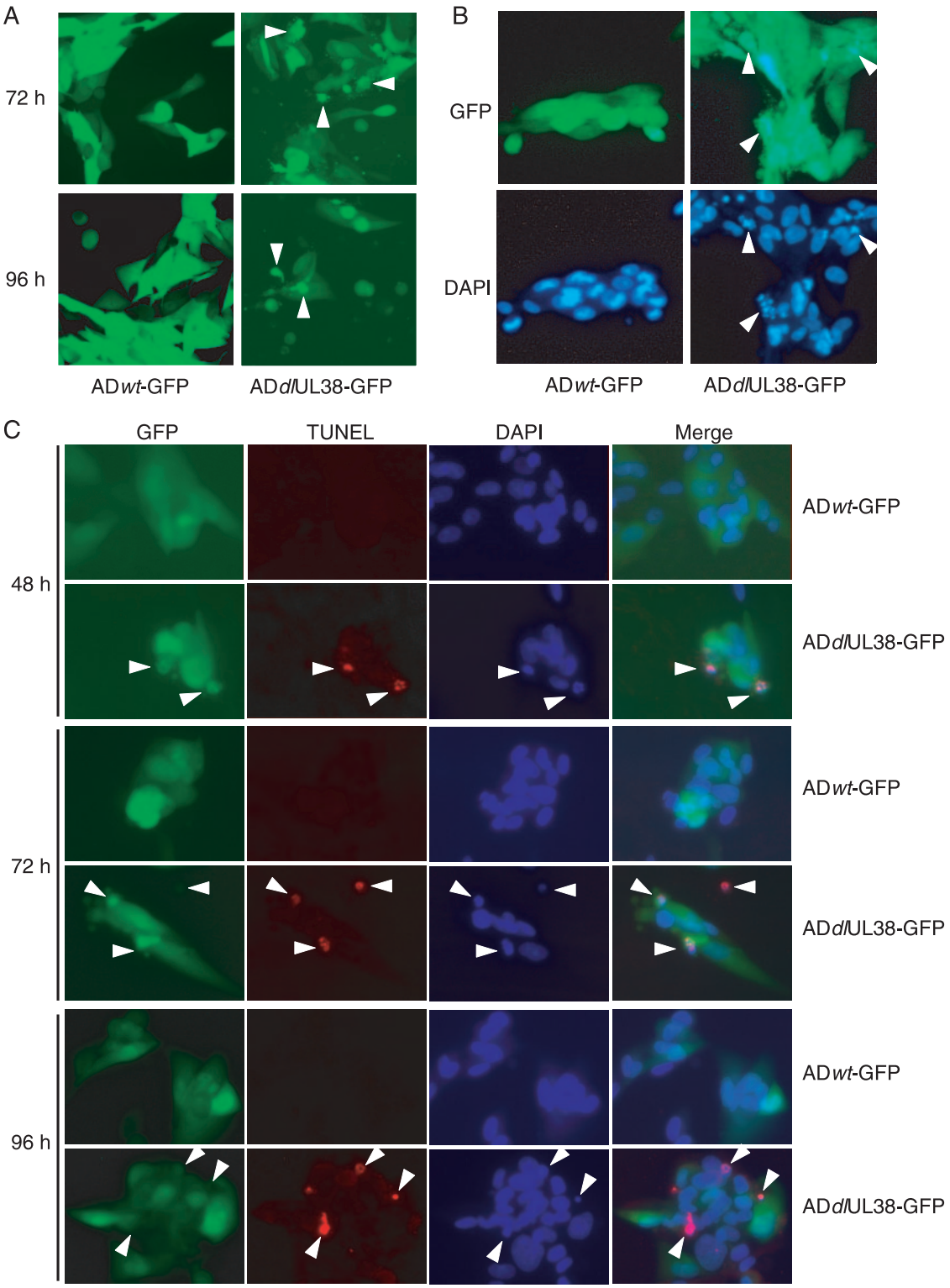

FIG. 6. Cells infected with the pUL38 deletion mutant demonstrate morphological changes characteristic of apoptosis. (A) Normal HF cells were infected with AD*wt*-GFP or AD*dl*UL38-GFP at an input genome number equivalent to 1 PFU of wild-type virus/cell, and the morphology of infected GFP-positive cells was examined under a fluorescence microscope at 72 h and 96 h postinfection. Arrowheads indicate representative cell shrinkage, membrane blebbing, and vesicle release in AD*dl*UL38-GFP infection. (B) Infected cells were labeled with DAPI at 96 h postinfection. Condensed chromatin in cells infected with AD*dl*UL38-GFP is indicated by arrowheads. (C) Infected cells were colabeled with DAPI and TUNEL at the indicated times postinfection. The colocalization of GFP, TUNEL, and DAPI staining in the same AD*dl*UL38-GFP-infected cell population is indicated.

enhanced rounding, shrinkage, and fragmentation. Quantitative analysis revealed that the cell loss started 24 h after infection with AD*dl*UL38 (Fig. 5A, right panel). Clearly, while wild-type virus effectively blocks the death of infected cells during the course of infection, AD*dl*UL38 induces extensive premature cell death, particularly at late times postinfection (16, 55).

We next tested whether the expression of pUL38 in *trans* restored cell viability during AD*dl*UL38 infection. pUL38-expressing cells (HF-UL38) or control cells (normal HF or HF-GFP cells) were infected with wild-type or mutant virus and examined microscopically (Fig. 5B, left panel), and cell numbers were counted (Fig. 5B, right panel) at 72 h postinfection. When infected with wild-type virus, HF-GFP cells and HF-UL38 cells showed almost identical morphologies, with no sign of excessive cell death. Similar to normal HF cells, HF-GFP cells infected with AD*dl*UL38 suffered extensive cell death, as evidenced by the presence of fewer attached cells and more rounded floating cells. In contrast, HF-UL38 cells were markedly resistant to cell death induced by AD*dl*UL38. The number of cells remaining attached to the culture dish was largely restored, and the overall morphology of AD*dl*UL38-infected HF-UL38 cells was nearly identical to that of AD*wt*-infected cells. Taken together, the induction of cell death by AD*dl*UL38 in normal or GFP-expressing fibroblasts and the inhibition of AD*dl*UL38-induced cell death by expression of pUL38 in *trans* demonstrate that pUL38 is required for the virus to inhibit cell death during infection.

Infection with pUL38 deletion virus induces morphological and biochemical events characteristic of apoptosis. The cell death observed during AD*dl*UL38 infection was accompanied by cell shrinkage and fragmentation, which are reminiscent of apoptosis. Consequently, we examined several characteristics of apoptosis in greater detail. We used the GFP-tagged UL38 mutant AD*dl*UL38-GFP and the wild-type control virus AD*wt*-GFP in this experiment in order to discriminate cells infected with the virus from uninfected cells and to visualize morphological details of infected cells by GFP expression. Normal HF cells were infected, and the morphology of GFP-positive cells was examined at 72 and 96 h postinfection, when extensive cell death became evident. At both times, many GFP-positive cells infected with AD*dl*UL38-GFP were rounded, had started to detach, and showed extensive cell shrinkage, membrane blebbing, and vesicle release (Fig. 6A). Furthermore, DAPI staining revealed that the chromatin of a substantial portion of the GFP-positive AD*dl*UL38-infected cells became condensed (Fig. 6B). All of these morphological changes are hallmarks of apoptosis. Most cells infected with AD*wt*-GFP maintained the typical morphology of HCMV-infected cells and showed no signs of cell rounding, shrinking, or detaching or chromatin condensation (Fig. 6A and B).

We used a TUNEL assay to measure nuclear DNA fragmentation, another indicator of apoptosis. HF cells were infected with AD*dl*UL38-GFP or AD*wt*-GFP and examined by TUNEL assay at various times postinfection (Fig. 6C). We detected little, if any, TUNEL staining in AD*wt*-GFP-infected cells. On the other hand, TUNEL-positive cells were evident after AD*dl*UL38-GFP infection, and the level of TUNEL staining increased during the course of infection. At late times (i.e., 72 h and 96 h postinfection), most of the apoptotic cells in AD*dl*UL38-GFP infection had already detached from the culture dish and therefore were not scored in the TUNEL assay, where only surface-attached cells were examined. Nevertheless, the assay clearly demonstrated extensive genomic fragmentation in attached cells infected with AD*dl*UL38-GFP, but not in cells infected with AD*wt*-GFP, at all times examined. The presence of GFP expression and TUNEL staining in the same cell population was readily observed at 48 h postinfection (Fig. 6C). Interestingly, at late times postinfection, while some of the TUNEL staining overlapped with a strong GFP signal, other TUNEL-positive cells exhibited a weak GFP signal. We interpret this observation to suggest that cells infected with AD*dl*UL38-GFP undergo apoptosis, generating apoptotic bodies that are TUNEL positive but losing the majority of cellular content due to compromised membrane integrity. Thus, the AD169 strain of cytomegalovirus lacking pUL38 induces cell death with characteristics of apoptosis.

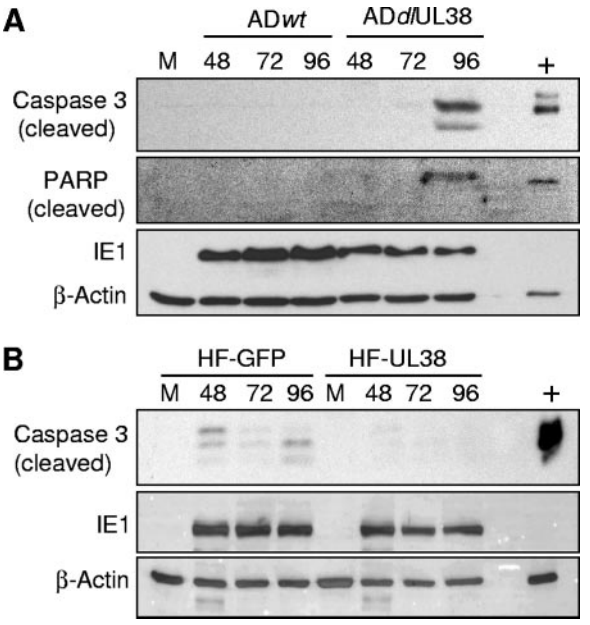

FIG. 7. AD*dl*UL38 induces elevated proteolytic cleavage of caspase 3 and PARP in HF cells. HF-GFP cells were infected with AD*wt* or AD*dl*UL38 at an input genome number equivalent to 1 PFU of wild-type virus/cell (A) or HF-GFP and HF-UL38 cells were infected with AD*dl*UL38 at an input genome number equivalent to 1 PFU of wild-type virus/cell (B), cells were collected at the indicated times postinfection, and cell lysates were examined for cleavage of caspase 3 and PARP by immunoblotting using monoclonal antibodies recognizing only the cleaved forms of the proteins. The infection control was IE1 expression, and the loading control was β-actin expression. Jurkat cell lysates treated with 0.25 mg/ml cytochrome *c* were used as the positive control for caspase 3 and PARP cleavage.

To determine whether biochemical markers of apoptosis were also induced by infection with the pUL38-deficient mutant, we examined the proteolytic cleavage of the main effector caspase, caspase 3, and one of its substrates, PARP, by Western blotting using monoclonal antibodies recognizing the cleaved forms. In normal HF cells and HF-GFP cells, AD*dl*UL38 induced the formation of multiple cleaved caspase 3 (~17/19 kDa) and PARP (89 kDa) products (Fig. 7A and data not shown). Although we observed caspase 3 cleavage starting at 48 h postin-

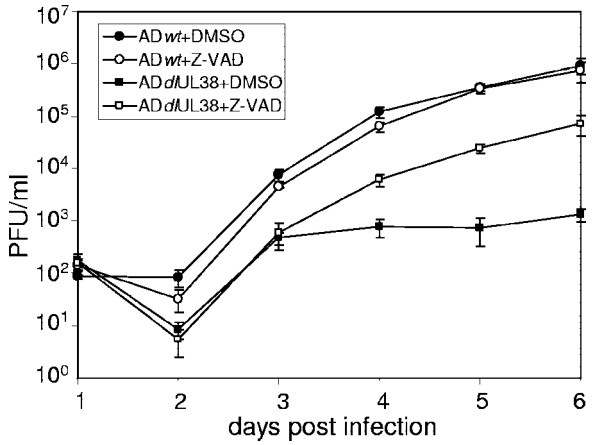

FIG. 8. Block of cell death by a caspase inhibitor largely restores the growth of AD*dl*UL38. Normal HF cells were infected with AD*wt* or AD*dl*UL38 at an input genome number equivalent to 2 PFU of wild-type virus/cell in the presence or absence of 100 μM Z-VAD-FMK. Culture media of infected cells were collected, and infected cells were supplemented with the appropriate Z-VAD-FMK- or DMSO-containing fresh medium every day for a total of 6 days postinfection. The DMSO-containing medium was used as the solvent control. Yields of cell-free virus were measure in duplicate by a plaque assay with HF-UL38 cells.

fection in some experiments (Fig. 7B), caspase 3 cleavage was generally most evident at late times postinfection (Fig. 7A). Induction of caspase 3 and PARP cleavage upon virus infection, however, was effectively blocked by the wild-type virus (Fig. 7A) or by expression of pUL38 in *trans* (Fig. 7B). Taken together, these results indicate that HCMV infection induces the caspase 3-dependent apoptosis pathway and that pUL38 is required to block these biochemical events. Collectively, our data suggest that pUL38 blocks caspase-dependent apoptosis and prevents premature cell death induced by virus infection.

Blocking apoptosis largely restores the growth defect of the pUL38 deletion virus. Deletion of the UL38 gene from the viral genome caused a $>10^5$-fold growth defect in the virus, and this defect resulted exclusively from the loss of the functional UL38 protein (Fig. 2). Additionally, AD*dl*UL38 induced apoptosis in infected cells, and virus-induced cell death was blocked by the expression of pUL38 in *trans* (Fig. 5 and 7). Consequently, we wanted to determine whether the defective growth of AD*dl*UL38 was a direct consequence of premature death of infected cells. Normal human fibroblasts were infected with pUL38-deficient or wild-type virus at an input genome number equivalent to 2 PFU wild-type virus/cell in the presence or absence of a broad-spectrum caspase inhibitor, Z-VAD-FMK, the culture medium was collected at various times thereafter, and extracellular virus yields were measured by a plaque assay (Fig. 8). In the absence of Z-VAD-FMK, there was a 1,000-fold difference in the peak yield of AD*dl*UL38 compared to that of wild-type virus. Treatment with Z-VAD-FMK had no effect on the growth of wild-type virus. In contrast, treatment with Z-VAD-FMK enhanced the peak yield of AD*dl*UL38 about 100-fold at day 6 postinfection and thus substantially restored its growth in normal human fibroblasts. This result suggests that premature death of infected cells by apoptosis is the main cause of the growth defect of AD*dl*UL38.

Overexpression of pUL38 in the absence of HCMV infection blocks apoptosis induced by multiple apoptotic stimuli. HCMV pUL38 might be a necessary and sufficient factor to inhibit cell death; alternatively, it is conceivable that pUL38 must interact with other viral proteins in order to prevent cell death in infected cells. To determine whether pUL38 has the intrinsic ability to block apoptosis in the absence of other HCMV proteins, we examined the responses of pUL38-expressing cells to multiple stimuli, including the mutant adenovirus *dl*337, anti-Fas antibody, and thapsigargin, which induce apoptosis through distinct modes. *dl*337 lacks the E1B-19K protein and induces caspase-dependent apoptosis through the intrinsic pathway in infected cells, which can be blocked by overexpression of the HCMV-encoded antiapoptotic protein pUL37x1, IE1, or IE2 and by the caspase inhibitor Z-VAD-FMK (13, 16, 34, 55; data not shown). While anti-Fas promotes apoptosis through the extrinsic pathway, thapsigargin induces the ER stress response and ultimately leads to ER-mediated cell death.

pUL38-expressing cells or control cells were infected with *dl*337, and cell death was monitored by morphological and quantitative analysis. Infection with *dl*337 rapidly induced cell death in HF-GFP cells, whereas HF-UL38 cells were markedly resistant (Fig. 9A, top panel). Quantitative analysis revealed that pUL38 protected cells from *dl*337-induced apoptosis for a wide range of input virus doses and times postinfection (Fig. 9A, middle and bottom panels). The ability of pUL38 to block *dl*337-induced cell death was not restricted to HF cells only. Two independently isolated HeLa cell lines stably expressing pUL38 were also markedly resistant to *dl*337-induced apoptosis (Fig. 9B). Moreover, HF-UL38 cells were also resistant to thapsigargin-induced caspase 3 cleavage and cell death compared to control cells (Fig. 10). On the other hand, pUL38 had little effect in protecting cells from apoptosis induced by anti-Fas (data not shown). Therefore, pUL38 is sufficient to block intrinsic and ER-mediated apoptosis induced by certain apoptotic agents in the absence of other viral proteins, but the protein appears not to be involved in the death ligand-induced extrinsic apoptosis pathway.

Taken together, we have demonstrated that the human cytomegalovirus UL38 protein is a cell death suppressor that inhibits caspase 3-dependent intrinsic and ER-mediated apoptosis and that blocking of premature cell death in infected cells by pUL38 is required for the optimal replication of AD169 in human fibroblasts.

DISCUSSION

The UL38 gene is a betaherpesvirus-specific gene; its homologs are present in human herpesvirus 6 and human herpesvirus 7. Furthermore, UL38 is well conserved among cytomegaloviruses of different species, such as primate cytomegaloviruses from chimpanzees and rhesus monkeys and nonprimate viruses from rats and mice (9, 14, 19, 37). A mutant virus lacking the entire pUL38 coding sequence, AD*dl*UL38, replicated its DNA inefficiently, grew poorly, and induced excessive death of infected HF cells (Fig. 2, 4, and 5). The infected cells showed morphological changes such as cell shrinkage, membrane blebbing, vesicle release, chromatin condensation, and fragmentation, all of which are characteristic of apoptosis (Fig. 5 and 6). A marker-rescued

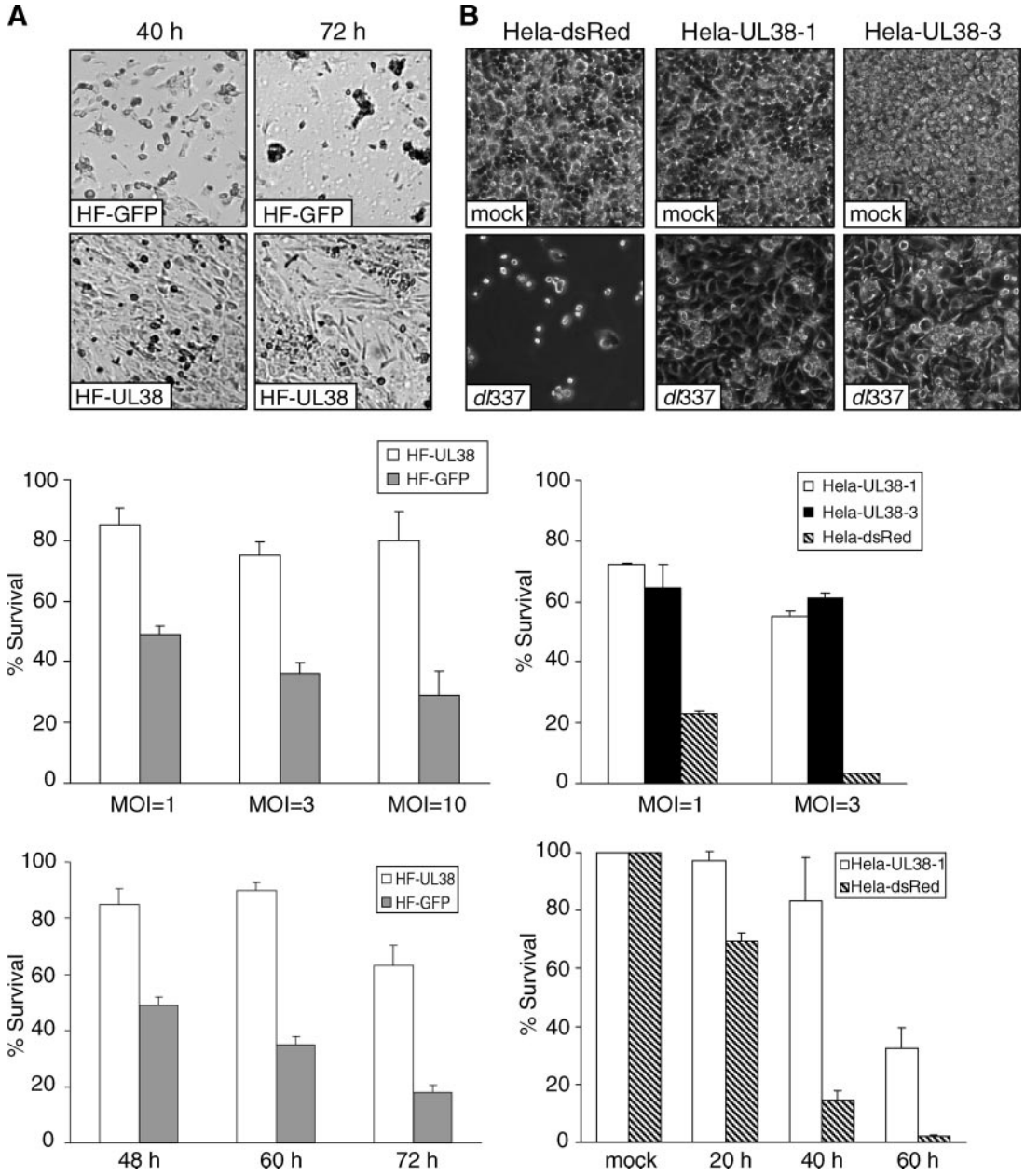

FIG. 9. Expression of pUL38 in *trans* blocks apoptosis induced by the mutant adenovirus *dl*337. (A) HF-GFP or HF-UL38 cells were infected with *dl*337. The morphology of infected cells was examined under a phase-contrast microscope (top panel, multiplicity of 3 PFU/cell), and the rate of cell death in *dl*337-infected cells was quantitated by labeling surviving cells with DAPI and counting DAPI-positive cells (middle panel, 48 h postinfection; bottom panel, multiplicity of 1 PFU/cell). Six independent fields for each sample were counted, and the number of cells in each *dl*337-infected HF-GFP or HF-UL38 sample was plotted as a percentage of that in a mock-infected sample. (B) HeLa cell lines stably expressing either the empty vector (HeLa-dsRed) or pUL38 (HeLa-UL38) were infected with *dl*337, the morphology of infected cells was examined under a phase-contrast microscope (top panel, multiplicity of 3 PFU/cell, 40 h postinfection), and the rate of cell death in *dl*337-infected cells was quantitated as described for panel A (middle panel, 40 h postinfection; bottom panel, multiplicity of 1 PFU/cell). Two independently isolated HeLa-UL38 cell lines (HeLa-UL38-1 and HeLa-UL38-3) were examined.

virus replicated indistinguishably from the wild type, and pUL38-expressing HF cells were resistant to cell death upon infection and effectively supported growth of AD*dl*UL38 (Fig. 2A and B and 5). Furthermore, caspase 3 and PARP were cleaved upon infection with AD*dl*UL38 in normal fibroblasts, and cleavage was blocked in pUL38-expressing HF cells (Fig. 7). Consistent with these observations, Z-VAD-FMK restored the growth of AD*dl*UL38 by a factor of 100 (Fig. 8). Thus, pUL38 functions to block apoptosis after HCMV infection. Finally, pUL38 acting in the absence of other HCMV gene products is sufficient to block apoptosis induced by infection with a mutant adenovirus that induces apoptosis and by thapsigargin, which induces ER-mediated cell death (Fig. 9 and 10).

The enhancement of the mutant virus yield by Z-VAD-FMK

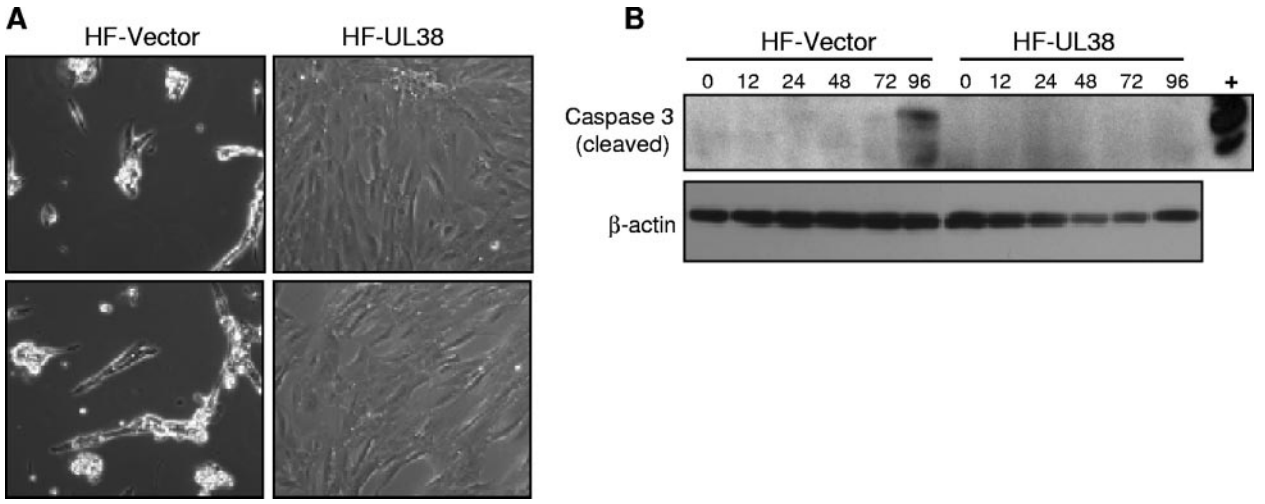

FIG. 10. Expression of pUL38 in *trans* blocks ER-mediated apoptosis induced by thapsigargin. pUL38-expressing cells (HF-UL38) or control cells (HF-vector) were treated with 2 μM thapsigargin. Cell morphology was examined under a phase-contrast microscope at 96 h posttreatment (A), and cleavage of caspase 3 was examined by immunoblotting (B). The loading control was β-actin expression. Jurkat cell lysates treated with 0.25 mg/ml cytochrome *c* were used as the positive control.

became evident at 72 to 96 h postinfection (Fig. 8), consistent with our observation that cell death in mutant-infected cells occurred late after infection. A 10-fold difference in cell-free virus yields for the mutant and the wild type, however, was still observed in the presence of Z-VAD-FMK. This difference in virus yields might represent the initial delay of the replication cycle of the mutant virus, as we did not pretreat cells with Z-VAD-FMK prior to infection. Alternatively, pUL38 might perform a function in addition to its role in blocking apoptosis.

We were able to rescue the AD*dl*UL38 virus by expressing pUL38 in *trans* (Fig. 2B). However, we observed some variation in the particle-to-PFU ratio among different mutant virus stocks prepared using different batches of pUL38-expressing fibroblasts. In a few cases, the difference was as much as 10-fold. The pUL38-expressing cells were not derived from a clonal cell line; rather, complementing cells comprise a heterogeneous pool of cells transduced with the pUL38-expressing retroviral vector. Consequently, the complementation ability of one batch of pUL38-expressing cells could differ significantly from that of another batch. Thus, the variation in the particle-to-PFU ratio is likely technical in nature and the result of the variable ability of different complementing cells to block cell death, which is required for efficient virus growth. It is conceivable that the failure to block cell death resulted in premature lysis of infected cells, and thus the release of various levels of immature virion particles or DNA-containing capsids, before virion assembly and egress were completed.

Multistep growth kinetic analysis indicated that expression of pUL38 in *trans* substantially enhances the growth of the pUL38 deletion virus. The $>10^5$-fold difference in peak yield of AD*dl*UL38 compared to that of wild-type virus in normal HF cells was reduced to 5-fold in HF-UL38 cells, which is comparable to the best case of *trans*-complementation for replication of a mutant HCMV deficient in an essential or augmenting gene that has been documented in the literature (Fig. 2B). Factors such as the heterogeneous nature of pUL38-expressing HF cells, as discussed above, or the less-than-optimal level and timing of pUL38 expression in these cells may contribute to the remaining fivefold growth reduction of the mutant virus in pUL38-expressing cells. Additionally, it is formally possible that UL38 deletion affects the expression of pUL37x1, the viral protein that has the antiapoptotic activity and is required for growth of the AD169 strain of HCMV. However, we previously isolated a mutant virus in which a transposon was inserted in the promoter region of UL37x1, resulting in a >90% expression reduction of pUL37x1 compared to wild-type virus, and the mutant virus grew at wild-type levels and showed no signs of apoptosis (51; data not shown). Furthermore, we and others recently showed that the pUL37x1 deletion AD169 virus failed to cause cell rounding and cytopathic effects compared to the wild-type virus. This was in striking contrast to the pUL38-deficient virus, which induced extensive cell rounding (Fig. 5) (36, 40). Interestingly, we found no evidence of apoptosis in cells infected with the UL37x1-deficient AD169 virus that expressed wild-type levels of pUL38 (40). Thus, the residual growth reduction of pUL38 deletion virus in HF-UL38 cells is likely technical in nature; the abilities of ectopically expressed pUL38 to support the growth of the pUL38 deletion virus (Fig. 2B) and to inhibit cell death as well as caspase 3 cleavage induced by the mutant virus (Fig. 5 and 7) indicate that pUL38 suppresses cell death and facilitates efficient virus replication.

UL38 is located in a complex transcription unit that also expresses the unspliced transcripts of UL36 and several variants of UL37 (Fig. 1A) (1, 16, 47). UL36, UL37, and UL37M are dispensable for virus infection in fibroblasts (6, 15, 16, 33, 51), and HCMV strain AD169 with a mutation in UL37x1 failed to replicate in human fibroblasts (38, 40, 51). Three tandemly arranged ORFs in this complex unit (UL36, UL37x1, and UL38), none of which share homology with known antiapoptosis proteins, are involved in the viral strategy to inhibit cell death. The UL36 and UL37x1 proteins are known as the viral inhibitor of caspase 8-induced apoptosis and the viral mitochondrial inhibitor of apoptosis (vMIA), respectively (for

a recent review, see reference 2). Furthermore, as noted above, the viral IE1 and IE2 proteins can also block apoptosis (21, 47, 49). It is evident that suppression of cell death is critical for the virus to complete its infection cycle and disseminate within the host, but the question remains regarding why the virus needs such an extensive arsenal to block a single cellular antiviral response.

It is possible that pUL36, pUL37x1, and pUL38 are required by the virus to inhibit cell death at different times during infection. pUL36 and pUL37x1 are expressed with immediate-early kinetics upon infection, whereas UL38 is an early gene that is expressed at both early and late times (33, 47) (Fig. 3). Cells infected with HCMV variants that express nonfunctional UL36 proteins due to spontaneous mutation were sensitive to Fas-mediated apoptosis within the first 48 h of infection, consistent with the immediate-early expression kinetics of UL36 (42). In our study, the UL38 mutant induced cell death mostly after 48 h postinfection, consistent with the early and late expression kinetics of UL38. It is also conceivable that pUL36, pUL37x1, and pUL38 function synergistically to maintain the viability of the host cell until the virus completes the infection cycle. This idea is consistent with the fact that the three gene products appear to block cell death induced through different mechanisms. It has been reported that UL36 prevents proteolytic activation of caspase 8 and blocks Fas-mediated extrinsic apoptosis, suggesting that UL36 might be involved in evading the host immune responses such as those mediated by cytotoxic T cells or natural killer cells (42). Overexpression of pUL37x1 disrupts the mitochondrial network, sequesters Bax at mitochondria, and subsequently prevents activation of caspase 9, thus blocking mitochondrion-mediated intrinsic apoptosis (3, 25, 35). However, an HCMV (Towne) mutant lacking pUL37x1 replicated efficiently and induced only a low level of caspase-independent cell death in infected cells, suggesting that the role of pUL37x1 in virus infection might differ from that observed in the overexpression setting (24). In this study, we demonstrated that the pUL38 deletion virus induces apoptosis in infected cells in the absence of any exogenous stimuli and that the function of pUL38 is to suppress caspase-dependent apoptosis in order for the virus to replicate efficiently. Furthermore, overexpression of pUL38 inhibits cell death induced by *dl*337 and thapsigargin but not that induced by anti-Fas, suggesting that pUL38 interferes with the intrinsic and ER-mediated pathways but plays little role in blocking the extrinsic apoptosis pathway. Therefore, it is intriguing to speculate that HCMV uses multiple viral products to achieve a complete blockage of programmed cell death, an innate antiviral response on which multiple signaling pathways converge, to maintain viability of the infected cell throughout the replication cycle.

It is noteworthy that the pUL37x1-deficient mutant of the AD169 strain of HCMV fails to replicate efficiently (38, 40), whereas a similar variant of the Towne strain of HCMV replicates normally (24). Although some variants of Towne contain functional UL36, AD169 contains an inactivating mutation in this antiapoptotic gene (42). Consequently, it is possible that the phenotype we observed for a pUL38-null mutant in an AD169 background would be masked in an HCMV strain that encodes an active gene product with a function redundant to that of pUL38.

Little is known at this point about the cellular target of pUL38 and the molecular mechanism of pUL38-mediated suppression of cell death. Even though pUL38 inhibits caspase-dependent cell death, it is entirely possible that pUL38 interferes with apoptotic signaling pathways that are not targeted by pUL36, pUL37x1, IE1, or IE2 or that pUL38 blocks the same pathways but engages them at a different step along the signaling cascade. Alternatively, pUL38 might be involved in blocking upstream signaling that leads to the onset of catalytic events of apoptosis rather than directly inhibiting enzymatic steps of the apoptotic cascade. Immunofluorescence analysis failed to reveal a colocalization of pUL38 with any cellular organelles (data not shown). Approaches directly examining interacting protein partners should provide insight into the mechanism of pUL38-mediated inhibition of cell death at the molecular level.

ACKNOWLEDGMENTS

We thank Herbert Virgin and the members of his laboratory for helpful discussions and invaluable advice, Te Tee Hong for excellent technical assistance, Joerg Schroeer for help with determining virus titers by IE1 expression, and Trish Robinson for assistance making the monoclonal anti-pUL38 antibody.

This work was supported by a Howard Temin award (CA-101957) from the National Cancer Institute (to D.Y.), a Public Health Service grant (AI-54430) from the National Institutes of Health (to T.S.), a grant-in-aid from the American Heart Association (0555636Z), a Wyeth young investigator award from the Infectious Diseases Society of America and the National Foundation for Infectious Diseases, and a grant from the American Cancer Society (IRG-58-010-48) (to D.Y.).

REFERENCES

1. **Adair, R., G. W. Liebisch, and A. M. Colberg-Poley.** 2003. Complex alternative processing of human cytomegalovirus UL37 pre-mRNA. J. Gen. Virol. **84:**3353–3358.
2. **Andoniou, C. E., and M. A. Degli-Esposti.** 2006. Insights into the mechanisms of CMV-mediated interference with cellular apoptosis. Immunol. Cell Biol. **84:**99–106.
3. **Arnoult, D., L. M. Bartle, A. Skaletskaya, D. Poncet, N. Zamzami, P. U. Park, J. Sharpe, R. J. Youle, and V. S. Goldmacher.** 2004. Cytomegalovirus cell death suppressor vMIA blocks Bax- but not Bak-mediated apoptosis by binding and sequestering Bax at mitochondria. Proc. Natl. Acad. Sci. USA **101:**7988–7993.
4. **Benedict, C. A., P. S. Norris, and C. F. Ware.** 2002. To kill or be killed: viral evasion of apoptosis. Nat. Immunol. **3:**1013–1018.
5. **Billstrom Schroeder, M., R. Christensen, and G. S. Worthen.** 2002. Human cytomegalovirus protects endothelial cells from apoptosis induced by growth factor withdrawal. J. Clin. Virol. **25**(Suppl. 2)**:**S149–S157.
6. **Borst, E. M., G. Hahn, U. H. Koszinowski, and M. Messerle.** 1999. Cloning of the human cytomegalovirus (HCMV) genome as an infectious bacterial artificial chromosome in *Escherichia coli*: a new approach for construction of HCMV mutants. J. Virol. **73:**8320–8329.
7. **Breckenridge, D. G., M. Germain, J. P. Mathai, M. Nguyen, and G. C. Shore.** 2003. Regulation of apoptosis by endoplasmic reticulum pathways. Oncogene **22:**8608–8618.
8. **Britt, W. J., and C. A. Alford.** 1996. Cytomegalovirus, p. 2493–2523. *In* B. N. Fields, D. M. Knipe, and P. M. Howley (ed.), Fields virology, 3rd ed. Lippincott-Raven Publishers, Philadelphia, PA.
9. **Brocchieri, L., T. N. Kledal, S. Karlin, and E. S. Mocarski.** 2005. Predicting coding potential from genome sequence: application to betaherpesviruses infecting rats and mice. J. Virol. **79:**7570–7596.
10. **Brune, W., C. Menard, J. Heesemann, and U. H. Koszinowski.** 2001. A ribonucleotide reductase homolog of cytomegalovirus and endothelial cell tropism. Science **291:**303–305.
11. **Cha, T. A., E. Tom, G. W. Kemble, G. M. Duke, E. S. Mocarski, and R. R. Spaete.** 1996. Human cytomegalovirus clinical isolates carry at least 19 genes not found in laboratory strains. J. Virol. **70:**78–83.
12. **Chee, M. S., A. T. Bankier, S. Beck, R. Bohni, C. M. Brown, R. Cerny, T. Horsnell, C. A. Hutchison III, T. Kouzarides, J. A. Martignetti, et al.** 1990. Analysis of the protein-coding content of the sequence of human cytomegalovirus strain AD169. Curr. Top. Microbiol. Immunol. **154:**125–169.
13. **Chiou, S. K., and E. White.** 1998. Inhibition of ICE-like proteases inhibits apoptosis and increases virus production during adenovirus infection. Virology **244:**108–118.

14. **Davison, A. J., A. Dolan, P. Akter, C. Addison, D. J. Dargan, D. J. Alcendor, D. J. McGeoch, and G. S. Hayward.** 2003. The human cytomegalovirus genome revisited: comparison with the chimpanzee cytomegalovirus genome. J. Gen. Virol. **84:**17–28.
15. **Dunn, W., C. Chou, H. Li, R. Hai, D. Patterson, V. Stolc, H. Zhu, and F. Liu.** 2003. Functional profiling of a human cytomegalovirus genome. Proc. Natl. Acad. Sci. USA **100:**14223–14228.
16. **Goldmacher, V. S., L. M. Bartle, A. Skaletskaya, C. A. Dionne, N. L. Kedersha, C. A. Vater, J. W. Han, R. J. Lutz, S. Watanabe, E. D. Cahir McFarland, E. D. Kieff, E. S. Mocarski, and T. Chittenden.** 1999. A cytomegalovirus-encoded mitochondria-localized inhibitor of apoptosis structurally unrelated to Bcl-2. Proc. Natl. Acad. Sci. USA **96:**12536–12541.
17. **Goodrum, F., C. T. Jordan, S. S. Terhune, K. High, and T. Shenk.** 2004. Differential outcomes of human cytomegalovirus infection in primitive hematopoietic cell subpopulations. Blood **104:**687–695.
18. **Grattan, M. T., C. E. Moreno-Cabral, V. A. Starnes, P. E. Oyer, E. B. Stinson, and N. E. Shumway.** 1989. Cytomegalovirus infection is associated with cardiac allograft rejection and atherosclerosis. JAMA **261:**3561–3566.
19. **Hansen, S. G., L. I. Strelow, D. C. Franchi, D. G. Anders, and S. W. Wong.** 2003. Complete sequence and genomic analysis of rhesus cytomegalovirus. J. Virol. **77:**6620–6636.
20. **Kinsella, T. M., and G. P. Nolan.** 1996. Episomal vectors rapidly and stably produce high-titer recombinant retrovirus. Hum. Gene Ther. **7:**1405–1413.
21. **Kovacs, A., M. L. Weber, L. J. Burns, H. S. Jacob, and G. M. Vercellotti.** 1996. Cytoplasmic sequestration of p53 in cytomegalovirus-infected human endothelial cells. Am. J. Pathol. **149:**1531–1539.
22. **Kuvin, J. T., and C. D. Kimmelstiel.** 1999. Infectious causes of atherosclerosis. Am. Heart J. **137:**216–226.
23. **Lukac, D. M., and J. C. Alwine.** 1999. Effects of human cytomegalovirus major immediate-early proteins in controlling the cell cycle and inhibiting apoptosis: studies with ts13 cells. J. Virol. **73:**2825–2831.
24. **McCormick, A. L., C. D. Meiering, G. B. Smith, and E. S. Mocarski.** 2005. Mitochondrial cell death suppressors carried by human and murine cytomegalovirus confer resistance to proteasome inhibitor-induced apoptosis. J. Virol. **79:**12205–12217.
25. **McCormick, A. L., V. L. Smith, D. Chow, and E. S. Mocarski.** 2003. Disruption of mitochondrial networks by the human cytomegalovirus UL37 gene product viral mitochondrion-localized inhibitor of apoptosis. J. Virol. **77:** 631–641.
26. **Melnick, J. L., E. Adam, and M. E. Debakey.** 1993. Cytomegalovirus and atherosclerosis. Eur. Heart J. **14**(Suppl. K)**:**30–38.
27. **Menard, C., M. Wagner, Z. Ruzsics, K. Holak, W. Brune, A. E. Campbell, and U. H. Koszinowski.** 2003. Role of murine cytomegalovirus US22 gene family members in replication in macrophages. J. Virol. **77:**5557–5570.
28. **Michaelis, M., R. Kotchetkov, J. U. Vogel, H. W. Doerr, and J. Cinatl, Jr.** 2004. Cytomegalovirus infection blocks apoptosis in cancer cells. Cell Mol. Life Sci. **61:**1307–1316.
29. **Mocarski, E. S., and C. T. Courcelle.** 2001. Cytomegaloviruses and their replication, p. 2629–2673. *In* D. M. Knipe, P. M. Howley, D. E. Griffin, R. A. Lamb, M. A. Martin, B. Roizman, and S. E. Straus (ed.), Fields virology, 4th ed., vol. 2. Lippincott-Raven, Philadelphia, PA.
30. **Muhlestein, J. B., B. D. Horne, J. F. Carlquist, T. E. Madsen, T. L. Bair, R. R. Pearson, and J. L. Anderson.** 2000. Cytomegalovirus seropositivity and C-reactive protein have independent and combined predictive value for mortality in patients with angiographically demonstrated coronary artery disease. Circulation **102:**1917–1923.
31. **Nakagawa, T., and J. Yuan.** 2000. Cross-talk between two cysteine protease families. Activation of caspase-12 by calpain in apoptosis. J. Cell Biol. **150:** 887–894.
32. **Nakagawa, T., H. Zhu, N. Morishima, E. Li, J. Xu, B. A. Yankner, and J. Yuan.** 2000. Caspase-12 mediates endoplasmic-reticulum-specific apoptosis and cytotoxicity by amyloid-beta. Nature **403:**98–103.
33. **Patterson, C. E., and T. Shenk.** 1999. Human cytomegalovirus UL36 protein is dispensable for viral replication in cultured cells. J. Virol. **73:**7126–7131.
34. **Pilder, S., J. Logan, and T. Shenk.** 1984. Deletion of the gene encoding the adenovirus 5 early region 1b 21,000-molecular-weight polypeptide leads to degradation of viral and host cell DNA. J. Virol. **52:**664–671.
35. **Poncet, D., N. Larochette, A. L. Pauleau, P. Boya, A. A. Jalil, P. F. Cartron, F. Vallette, C. Schnebelen, L. M. Bartle, A. Skaletskaya, D. Boutolleau, J. C. Martinou, V. S. Goldmacher, G. Kroemer, and N. Zamzami.** 2004. An anti-apoptotic viral protein that recruits Bax to mitochondria. J. Biol. Chem. **279:**22605–22614.
36. **Poncet, D., A. L. Pauleau, G. Szabadkai, A. Vozza, S. R. Scholz, M. Le Bras, J. J. Briere, A. Jalil, R. Le Moigne, C. Brenner, G. Hahn, I. Wittig, H. Schagger, C. Lemaire, K. Bianchi, S. Souquere, G. Pierron, P. Rustin, V. S. Goldmacher, R. Rizzuto, F. Palmieri, and G. Kroemer.** 2006. Cytopathic effects of the cytomegalovirus-encoded apoptosis inhibitory protein vMIA. J. Cell Biol. **174:**985–996.
37. **Rawlinson, W. D., H. E. Farrell, and B. G. Barrell.** 1996. Analysis of the complete DNA sequence of murine cytomegalovirus. J. Virol. **70:**8833–8849.
38. **Reboredo, M., R. F. Greaves, and G. Hahn.** 2004. Human cytomegalovirus proteins encoded by UL37 exon 1 protect infected fibroblasts against virus-induced apoptosis and are required for efficient virus replication. J. Gen. Virol. **85:**3555–3567.
39. **Sagara, Y., F. Fernandez-Belda, L. de Meis, and G. Inesi.** 1992. Characterization of the inhibition of intracellular Ca^{2+} transport ATPases by thapsigargin. J. Biol. Chem. **267:**12606–12613.
40. **Sharon-Friling, R., J. Goodhouse, A. M. Colberg-Poley, and T. Shenk.** 2006. Human cytomegalovirus pUL37x1 induces the release of endoplasmic reticulum calcium stores. Proc. Natl. Acad. Sci. USA **103:**19117–19122.
41. **Silva, M. C., Q. C. Yu, L. Enquist, and T. Shenk.** 2003. Human cytomegalovirus UL99-encoded pp28 is required for the cytoplasmic envelopment of tegument-associated capsids. J. Virol. **77:**10594–10605.
42. **Skaletskaya, A., L. M. Bartle, T. Chittenden, A. L. McCormick, E. S. Mocarski, and V. S. Goldmacher.** 2001. A cytomegalovirus-encoded inhibitor of apoptosis that suppresses caspase-8 activation. Proc. Natl. Acad. Sci. USA **98:**7829–7834.
43. **Smith, G. A., and L. W. Enquist.** 1999. Construction and transposon mutagenesis in *Escherichia coli* of a full-length infectious clone of pseudorabies virus, an alphaherpesvirus. J. Virol. **73:**6405–6414.
44. **Speir, E., R. Modali, E. S. Huang, M. B. Leon, F. Shawl, T. Finkel, and S. E. Epstein.** 1994. Potential role of human cytomegalovirus and p53 interaction in coronary restenosis. Science **265:**391–394.
45. **Streblow, D. N., S. L. Orloff, and J. A. Nelson.** 2001. Do pathogens accelerate atherosclerosis? J. Nutr. **131:**2798S–2804S.
46. **Tanaka, K., J. P. Zou, K. Takeda, V. J. Ferrans, G. R. Sandford, T. M. Johnson, T. Finkel, and S. E. Epstein.** 1999. Effects of human cytomegalovirus immediate-early proteins on p53-mediated apoptosis in coronary artery smooth muscle cells. Circulation **99:**1656–1659.
47. **Tenney, D. J., and A. M. Colberg-Poley.** 1991. Expression of the human cytomegalovirus UL36-38 immediate early region during permissive infection. Virology **182:**199–210.
48. **Terhune, S. S., J. Schroer, and T. Shenk.** 2004. RNAs are packaged into human cytomegalovirus virions in proportion to their intracellular concentration. J. Virol. **78:**10390–10398.
49. **Tullis, G. E., and T. Shenk.** 2000. Efficient replication of adeno-associated virus type 2 vectors: a *cis*-acting element outside of the terminal repeats and a minimal size. J. Virol. **74:**11511–11521.
50. **Varnum, S. M., D. N. Streblow, M. E. Monroe, P. Smith, K. J. Auberry, L. Pasa-Tolic, D. Wang, D. G. Camp II, K. Rodland, S. Wiley, W. Britt, T. Shenk, R. D. Smith, and J. A. Nelson.** 2004. Identification of proteins in human cytomegalovirus (HCMV) particles: the HCMV proteome. J. Virol. **78:**10960–10966.
51. **Yu, D., M. C. Silva, and T. Shenk.** 2003. Functional map of human cytomegalovirus AD169 defined by global mutational analysis. Proc. Natl. Acad. Sci. USA **100:**12396–12401.
52. **Yu, D., G. A. Smith, L. W. Enquist, and T. Shenk.** 2002. Construction of a self-excisable bacterial artificial chromosome containing the human cytomegalovirus genome and mutagenesis of the diploid TRL/IRL13 gene. J. Virol. **76:**2316–2328.
53. **Yu, Y., and J. C. Alwine.** 2002. Human cytomegalovirus major immediate-early proteins and simian virus 40 large T antigen can inhibit apoptosis through activation of the phosphatidylinositide 3′-OH kinase pathway and the cellular kinase Akt. J. Virol. **76:**3731–3738.
54. **Zhou, Y. F., M. B. Leon, M. A. Waclawiw, J. J. Popma, Z. X. Yu, T. Finkel, and S. E. Epstein.** 1996. Association between prior cytomegalovirus infection and the risk of restenosis after coronary atherectomy. N. Engl. J. Med. **335:**624–630.
55. **Zhu, H., Y. Shen, and T. Shenk.** 1995. Human cytomegalovirus IE1 and IE2 proteins block apoptosis. J. Virol. **69:**7960–7970.